Determination of Photometric Properties of Materials for Energy Purposes Through the Experimental Study of a Two-Axis Goniophotometer

Roberto de Lieto Vollaro[#1], Giovanni Demegni[#2], Emiliano Carnielo[#3], Fabio Botta[#4], Emanuele de Lieto Vollaro[#5]

[#] Department of Engineering, Università degli studi Roma Tre, Via della Vasca Navale 79, Rome - 00146, Italy
[1]roberto.delietovollaro@uniroma3.it
[2]giovannidemegni@gmail.com
[3]emiliano.carnielo@gmail.com
[4]fabio.botta@uniroma3.it
[5]emanuele.delieto@gdfsuez.com

***Abstract*— A two-axis scanning goniophotometer has been designed and developed at LIFT (Laboratorio Ingegneria Fisica Tecnica) at Engineering Department, University of Roma Tre (Rome) and the data compared with those obtained from the video-projection goniophotometer at an important national Institute of Metrology. By this instrument a correlation between the reflectance and the angle of incidence will be propoposed. This function is useful for all the programs that simulates the dynamics of the energy systems in buildings where, typically, the reflectance is approximated by a constant, overestimating the values of the solar gains.**

Keywords: Goniophotometer, Solar Gains, Reflectance, BRDF

Nomenclature

Symbols		Subscript	
E	Illuminance $[lux]$	$beam$	direct
I	Solar Radiation $\left[W/_{m^2}\right]$	d	average value
L	Luminance $\left[cd/_{m^2}\right]$	$diff$	diffusive
M	Emittance $[lux]$	i	incidence
q	Radiance coefficient []	r	reflection
Q	Solar Gain $\left[W/_{m^2}\right]$	t	transmitted
ρ	Reflectance $[-]$	v	fotometric
ω	Solid Angle $[sr]$		
ϕ	Luminous Flux $[lm]$		
$\varphi_{t(r)}$	Azimuthal angle		
$\theta_{t(r),}$	Zenithal angle		
$\theta_{i,}\varphi_i$	angles of incidence of incoming radiation illuminating		

I. INTRODUCTION

Most goniophotometers measure, onto a sample of interest, the transmitted, reflected or radiance luminance in a direction relative to the incident or irradiance illuminance from another direction (Andersen and de Boer 2006 [2]). The data measured by goniophotometers are epitomized by theBT(R)DF: Bi-directional Transmission (or Reflection) Distribution Function defined by the Commission Internationale de l'Eclairage as the ''quotient of the luminance of the medium by the illuminance on the medium'' (CIE 1977). This function can be described matematically as follows:

$$BT(R)DF_v\left(\theta_{t(r),}\varphi_{t(r)},\theta_{i,}\varphi_i\right) = \frac{L_v(\theta_{t(r)},\varphi_{t(r)},\theta_{i,}\varphi_i)}{E_v(\theta_i)} \qquad [sr^{-1}]$$

where $\theta_{t(r)}, \varphi_{t(r)}$ are the zenithal and azimuthal angles of emergence of transmitted (or reflected) radiation, $\theta_{i,}\varphi_i$ are the angles of incidence of incoming radiation illuminating a sample, L_v is the luminance of transmitted (reflected) light and E_v is the illuminance of the incoming radiation.

II. INSTRUMENT DESIGN

A two-axis scanning goniophotometer for measuring the spatial distribution of light outcoming from materials used has been designed by LIFT at Roma Tre (Fig. 1). To take the measures the sample is kept stationary at the center of the goniometer and the photometer head is turned around it ([9] – [11]).

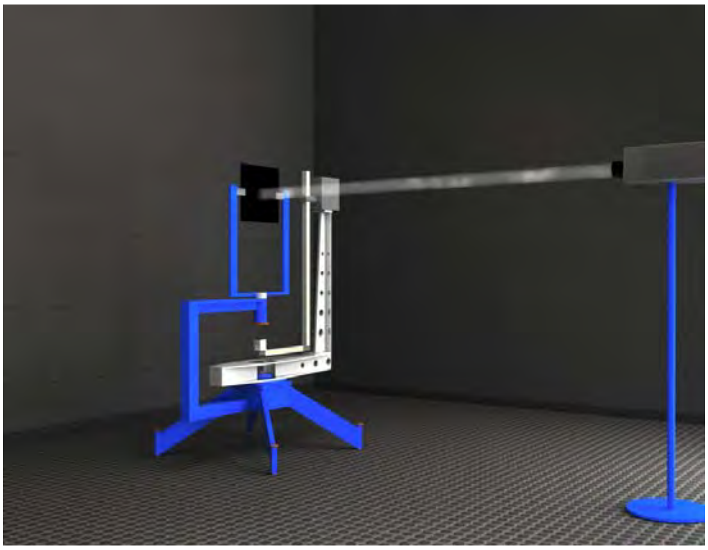

Fig. 1. Rendering of the two-axis scanning goniophotometer designed to measure BT(R)DF

The goniophotometer system is run in the laboratory, environmental conditions of which are under control, the walls and the ceiling of which are finished in matt black paint. The components of the goniophotometer are: a goniometer having two AC induction motor controlled arms, height and angular adjustable sample holder, and the photometer head having a luxmeter and a a 400W Halogen Lamp with an optical system of focusing lens used as incoming beam. The goniometer is made up of a mounting-base, a computer-controlled outer arm coupled to the mounting-base and a computer-controlled interior arm coupled to the outer arm. The mounting-base is equipped with four adjustable legs which are used for keeping the goniometer in balance and to in a vibration-free condition. The L-shaped goniometer arms moves in azimuthal angles (φ) from 0° to 160° the outer while the interior is used for assembling the photometer head and scanning of the emitting sample within the polar angles (θ) from 0° to 360°.

III. COMPARING EXPERIMENTAL RESULTS

Both for the measurements conducted at Institute Of Metrology, with a video-projection goniophotometer, that for ones carried on RomaTre, the characterization of the surface of the materials was conducted investigating the reflective properties on the plane swept by the inner arm along the meridian that corresponds to the position of 80° of the outer arm (Fig. 3).

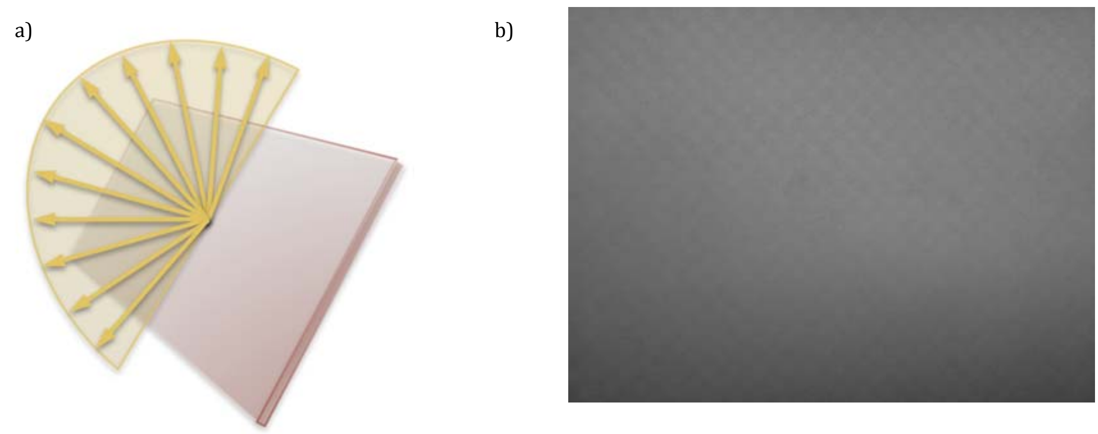

Fig. 2. a) Reference System for acquiring data. In light red the sample while the arrows represent the scanned plane of the outcoming radiation. b) Sample of material made of roof sheathing with a 45° texture.

Following are the results in polar coordinates obtained for the position of the sample at 8° , respectively for "LIFT" and "Institute Of Metrology".

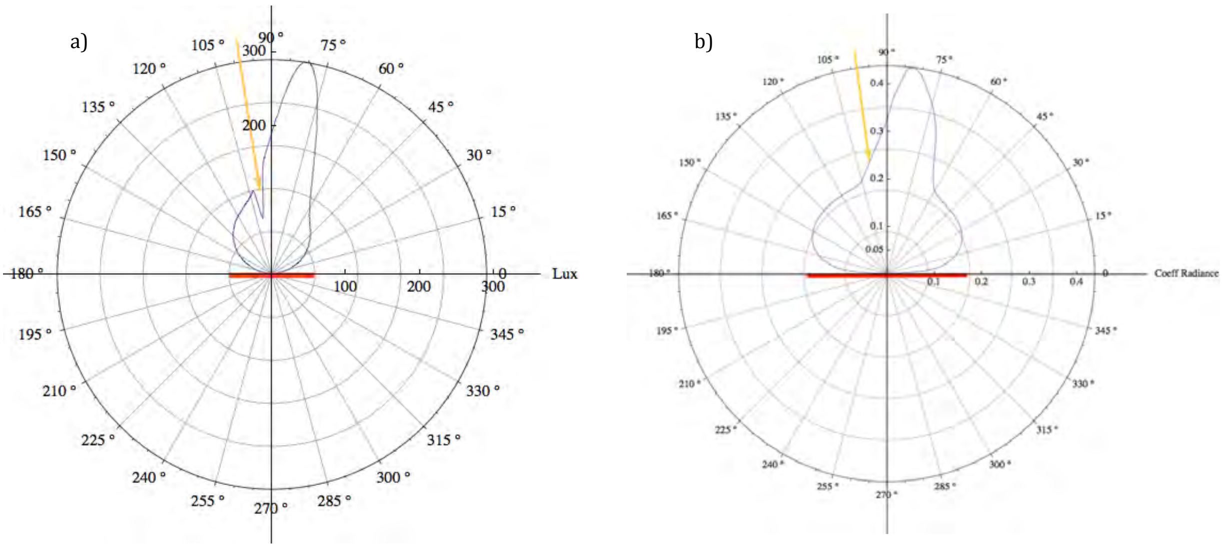

Fig. 3. a) Luminous Emittance. LIFT. b) BRDF evaluated at INSTITUTE OF METROLOGY

Trends of the two graphs are only apparently different, in fact they represent different quantities: the coefficient of radiance that q ($BRDF$) evaluated at Institute Of Metrology is defined as:

$$q = \frac{L_{v,reflected}}{E_v(\theta_{incident})}$$

while the Luminous Emittance M_v evaluated at Rome is::

$$M_v = \frac{d\phi_v}{dA}$$

which differs from the Luminance reflected L_v :

$$L_{v,reflected} = \frac{d^2\Phi_v}{(dA \cdot d\omega \cdot cos\theta)}$$

for the infinitesimal solid angle and for the projection of the element of the surface investigated in the direction of observation. In order to make a comparison we observe that $L_{v,reflected}$ can be written as :

$$L_{v,reflected} = M_v \cdot \frac{d\phi_v}{d\omega} \cdot \frac{1}{\cos\theta}$$

and considering $E_v(\theta_{incident})$ and ${}^{d\phi_v}/_{d\omega}$ scale factors we have:

$$q = M_v \frac{1}{E_v} \frac{d\Phi_v}{d\omega} \frac{1}{\cos\theta}$$

thus being able to obtain the Emittance M_v and compare graphs:

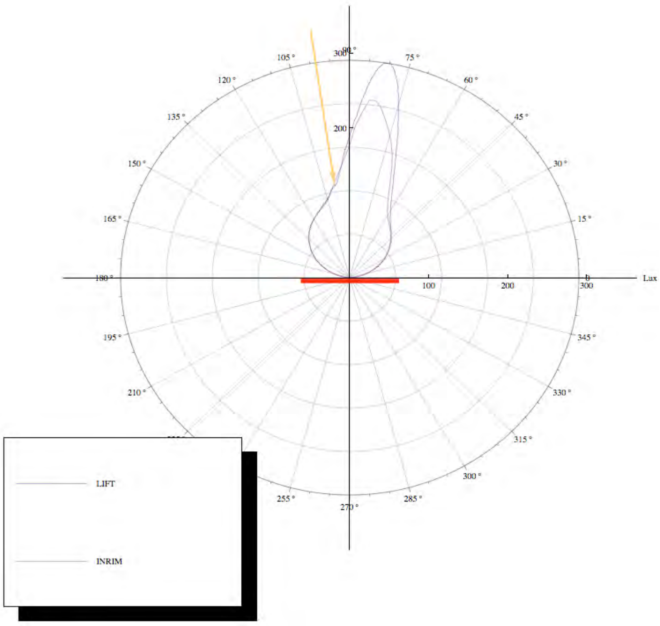

Fig. 4. Comparison between LIFT's Emittance and Institute Of Metrology's Emittance

The graphs illustrate the diffusive zone and the reflecting zone in specular direction. Through an interpolation process (both for Institute Of Metrology and LIFT) the trends were corrected for degrees eclipsed by the movement of inner arm The trends are similar and the differences are within the accepted experimental errors.. The different magnitude reached in the reflective area depends on different values of illuminance due to different light sourced used: Institute Of Metrology saturated the sensor distorting the peak zone, obtained later via an algorithm.

IV. Measurement of integrated values of the angular reflectance

The reflectance ρ is defined as the ratio between the reflected radiant flux and the incident flux:

$$\rho = \frac{d\phi_r}{d\phi_i}$$

Indicating with ϑ_r and ϑ_i the angle of the reflection and incidence respectively we obtain ([3], [4]) $d\phi_{reflected} = dL_r \cdot dA \cdot \cos\vartheta_r$, $d\phi_{incident} = dL_i \cdot dA \cdot \cos\vartheta_i$ and the reflectance can be written as:

$$\rho(\vartheta_i, \vartheta_r) = \frac{dL_r}{dL_i \cdot dA \cdot \cos\vartheta_i} \cdot dA \cdot \cos\vartheta_r = q \cdot \cos\vartheta_r$$

where $\rho(\vartheta_i, \vartheta_r)$ provides the reflectance for the angles of reflection ϑ_r and incidence ϑ_i. Calculating its average value on π (considering a plan hemisphere) or on 2π (for the entire hemisphere), we obtain:

$$\bar{\rho}_{(\vartheta_i)} = \frac{1}{2\pi} \int_0^{2\pi} q \cdot \cos \vartheta_r \cdot d\omega$$

This value therefore, providing for the necessary normalization of the coefficients a 1, indicates the percentage of reflected radiation from the surface of the material when the incidence beam defines with the surface normal the ϑ_i angle. Therefore it was assessed the reflectance $\bar{\rho}_{(\vartheta_i)}$ for areas at each angle of incidence of the beam of 8° (see Figure 5), generating values [12,13].

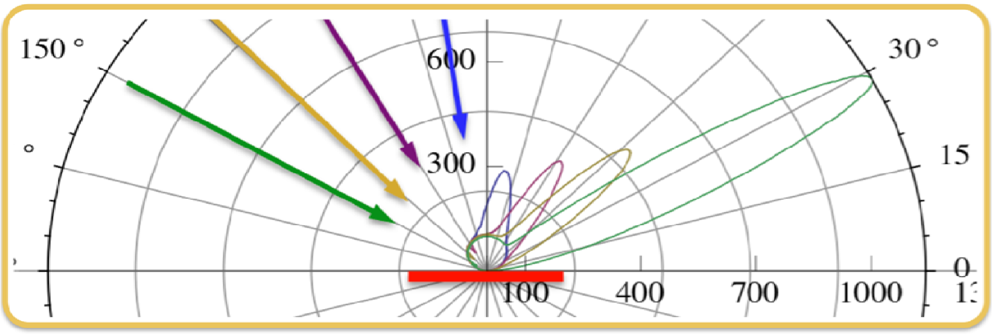

Fig. 5. Area Increasing Progression of Reflectance with angle

Interpolating with a second order polynomial regression the obtained it was extrapolated the polynomial to better approximate the data (Fig. 6).

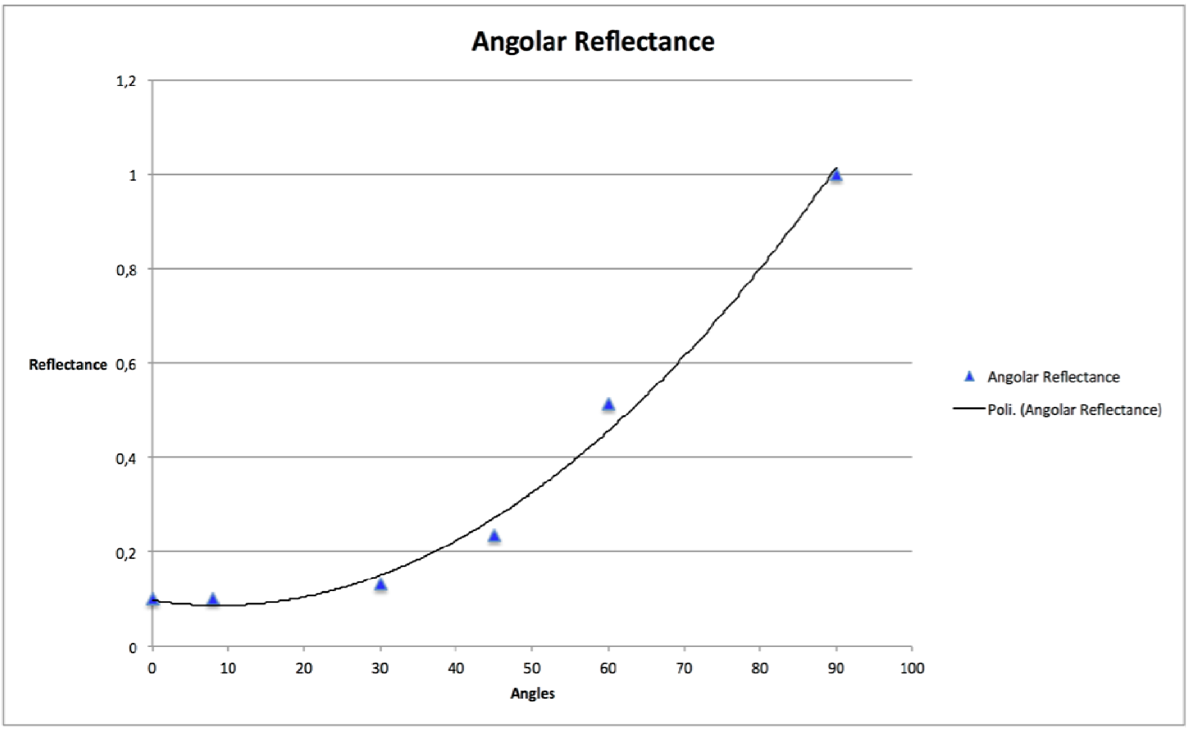

Fig. 6. Trend curve of growth for Angular Reflectance

V. Energetic Simulation

To study the influence of the dependency of reflectance with the angle of incidence on the solar gains a comparison has been done. The solar gain can be written as:

$$Q_{sg} = (I_{beam} + I_{diff}) \cdot (1 - \rho) \qquad \left[\frac{W}{m^2}\right]$$

where I_{beam} is the direct radiation incident per unit area and I_{diff} indicates the diffuse radiation incident per unit area. Considering a horizontal surface (the roof of a building for example) on the one hand the simulations ρ=cost were conducted using the platform TRNSYS® Simulation Studio, on the other hand, the trend curve of angular reflectance was incorporated

$$Q^*{}_{sg} = \left[I_{beam} \cdot \left(1 - \rho(\vartheta)\right) + I_{diff} \cdot (1 - \rho_d)\right] \qquad \left[\frac{W}{m^2}\right]$$

where $\rho_d = \frac{1}{\pi/2} \cdot \int_0^{\pi/2} \rho(\vartheta)\, d\vartheta$ represent the average value

The two curves of solar gains were calculated for January 1st and July 1st, plotting also the contribution of total incident radiation in light green, as shown in Figure 7 and 8:

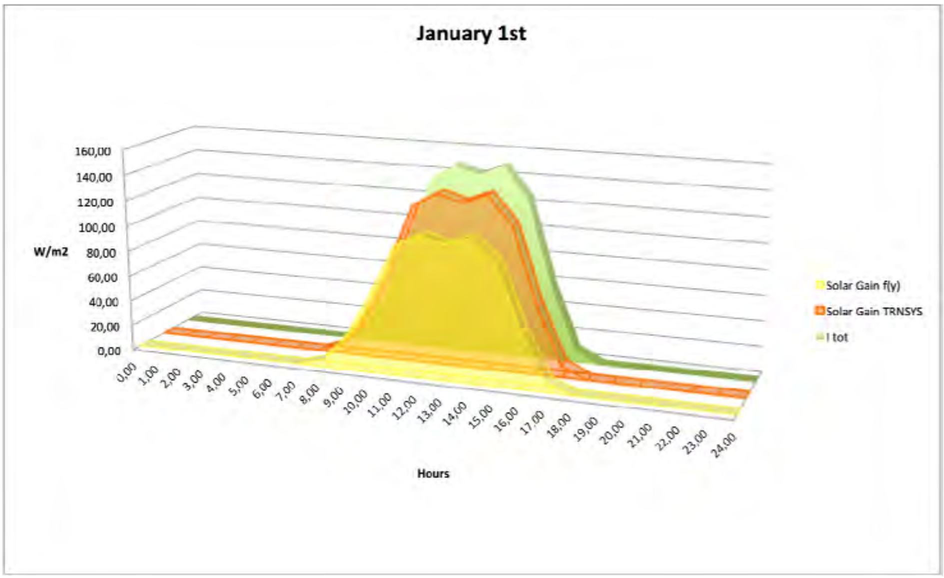

Fig. 7 Comparing Solar Gains for 1st of July

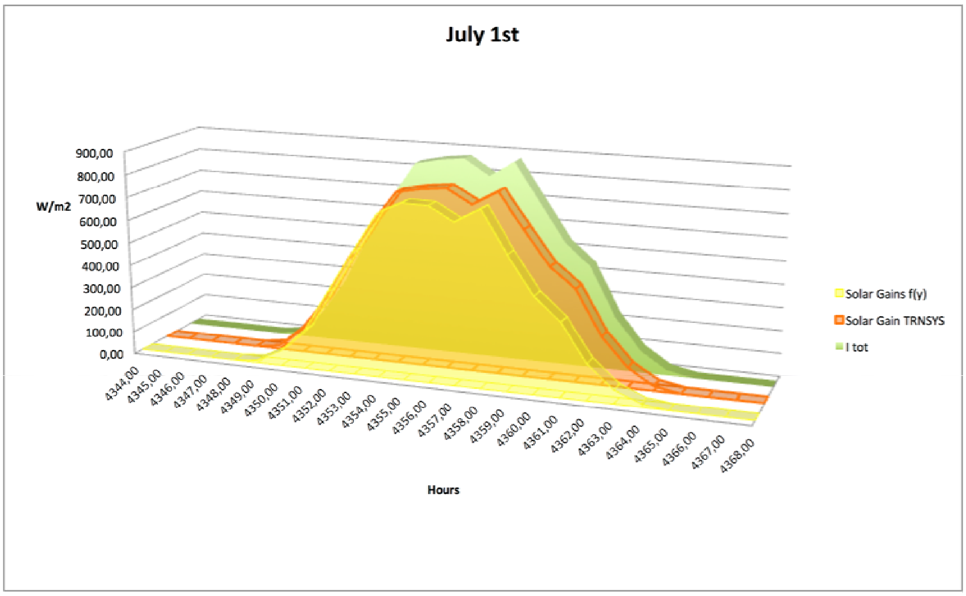

Fig. 8. Comparing Solar Gains for 1st of January

The graphs show how in both cases the values of solar gains, calculated considering a variable trend of the reflectance coefficient, are lower than those calculated with.ρ=cost. The difference also grows up conducting extensive tests not only to a horizontal surface but also considering the contributions on vertical surfaces [6,7].

VI. CONCLUSION

The spatial distribution of the value of Luminous Emittance M_v measured with the two-axis scanning goniophotometer designed at LIFT, allowed to evaluate the performance of the BRDF for a semi-specular surface. The comparison with the measurements obtained by a video-projection goniophotometer at Institute Of Metrology granted their repeatability. A function that correlates the reflectance with the angle of incidence has been proposed. This information represents an innovation for the dynamic simulation software of energy systems in buildings, which approximates the trend of the reflectance at a constant value ([5], - [8]). The comparison conducted by placing this information revealed an overestimation of solar gains by the software.

Future developments of this study relate to the optimization of the sensor, with the installation of the luminance meter in place of the luxmeter, with the aim to extend the range of the estimated frequencies measured. In this manner we will be able to evaluate the behavior of the opaque and transparent materials also in the infrared range to better estimate their optical characteristics. Moreover studies about more complex system, like the surfaces of an urban public transport, have been planned with the aim to optimize their performances ([15])

REFERENCES

[1] M. Andersen, M. Rubin, R. Powles and J.-L. Scartezzini, “Bidirectional transmission properties of Venetian blinds: experimental assessment compared to ray-tracing calculations,” *Solar Energy*, 78, pp. 187-198, 2005.

[2] M. Andersen and J. de Boer, “Goniophotometry and assessment of bidirectional photometric properties of complex fenestration systems,” *Energy and Buildings*, 38, pp. 836-848, 2006.

[3] W. Erb, “Computer-controlled gonioreflectometer for the measurement of spectral reflection characteristics,” *Applied Optics*,Vol. 19, No. 22, 1980.

[4] P. Apian-Bennewitz, “Designing an apparatus for measuring bidirectional reflection/transmission,” *Proc. Optical Materials Technology for Energy Efficiency and Solar Energy Conversion XIII*, SPIE, April 1994, vol. 2255, pp. 697-706.

[5] “2006 Buildings Energy Databook”, http://buildings databook.eren.doe.gov/docs/1.1.3.pdf (accessed 4-13-07), September 2006, U.S. Department of Energy

[6] M. Kischkoweit-Lopin. “An Overview of Daylighting Systems”, Solar Energy Vol. 73 No. 2, pp. 77-82, 2002.

[7] H. Koster. Dynamic Daylighting Architecture: Basics, Systems, Projects. August 1, 2004, Birkhauser

[8] R. Sullivan, L. Beltran, E.S. Lee, M. Rubin, and S.E.Selkowitz. “Energy and Daylight Performance of Angular Selective Glazings”, proceedings of the ASHRAE/DOE/BTECC Conference, December 7-11 1998

[9] M. Andersen, J. de Boer. “Goniophotometry and assessment of bidirectional photometric properties of complex fenestration systems”, Energy and Buildings 38 (2006) 836-848

[10] G.J. Ward, “Measuring and modeling anisotropic reflection”, ACM SIGGRAPH Comput Graphics 26 (2) (1992) 265-272

[11] P. Apian-Bennewitz. “pab Gonio-Photometer II”,http://www.pab-opto.de/gonio-photometer/ (accessed 4-14-07), 2007, pab-opto consultancy

[12] M. Andersen, C. Roecker, J.L. Scartezzini. “Design of a time-efficient video-goniophotometer combining bidirectional functions assessment for transmission and reflection”, Solar Energy Materials and Solar Cells 88 (2005) 97-118

[13] C. Browne. “Development of a light detection system for bidirectional measurements over the solar spectrum and sun course simulations with Scale Models”, June 5, 2006. Massachusetts Institute of Technology

[14] M. Andersen, D. Ljubicic, C. Browne, S. Kleindienst, M. Culpepper. “Automated Assessment of Light Redirecting Properties of Materials and Sunlight Penetration within Scale Models: The Heliodome Project”. Proceedings of the ISES 2005 Solar World Congress, August 8-12, 2005

[15] R. De Lieto Vollaro, F. Botta, L. Evangelisti, P. Gori, C. Guattari, “Energy Performance Optimization of a Bus for Urban Public Transport,” International Journal of Engineering and Technology Vol. 5, No 4, pp. 3639-3648.